Artificially Structured Thin-Film Materials and Interfaces

V. NARAYANAMURTI

The ability to artificially structure new materials on an atomic scale by using advanced crystal growth methods such as molecular beam epitaxy and metal-organic chemical vapor deposition has recently led to the observation of unexpected new physical phenomena and to the creation of entirely new classes of devices. In particular, the growth of materials of variable band gap in technologically important semiconductors such as GaAs, InP, and silicon will be reviewed. Recent results of studies of multilayered structures and interfaces based on the use of advanced characterization techniques such as high-resolution transmission electron microscopy and scanning tunneling microscopy will be presented.

ADVANCES IN SOLID-STATE ELECTRONICS CAN USUALLY BE traced to a combination of new concepts, materials, and device principles. Integrated circuits, for example, were made possible by the discovery of zone refining, which made possible the synthesis of ultrapure bulk silicon and germanium.

A number of spectacular advances have been made in constructing new materials (*1*) by ultrahigh vacuum and vapor-phase crystal growth techniques. New combinations of materials called heterostructures can be made that have an artificial periodicity and structure which can be controlled at the atomic level. These novel materials include a variety of combinations of metals, semiconductor, and insulators. Quantum mechanical effects can be seen in these thin films and heterostructures, which have dimensions of only a few hundred angstroms. Thus, one can investigate experimentally the one-dimensional quantization of electrons that is familiar to undergraduate physics students. The quantum tunneling of electrons across such thin films can be observed when the thickness of the films is comparable to the extension of electronic wave functions (10 to 100 Å). The control of the electronic and optical properties of materials at the quantum level will have a major impact on new technology, particularly in the area of optoelectronics (*2*). Although much work has been done recently in the area of metal films (*3*), this article will be confined to a discussion of progress in the area of thin-film semiconductor structures grown on technologically important materials such as GaAs, InP, and silicon.

Semiconductor Heterostructures and Epitaxy

A semiconductor film grows epitaxially if the crystallinity and orientation of the deposited layer are determined by the substrate. If the single crystal formed consists of thin films of dissimilar semiconductors one on top of the other, then the process is called heteroepitaxy. Heteroepitaxy provides new degrees of freedom on the surface of a semiconductor. Although the dominant material in semiconductor electronics has been silicon, researchers are striving to improve its electronic properties through controlled changes in the band structure of the material. For example, compound semiconductors such as GaAs have an intrinsically higher electron mobility than silicon. More importantly, unlike silicon, many III-V semiconductors (semiconductors made from elements in groups III and V, for example, GaAs) have direct energy band gaps that facilitate the efficient recombination of electrons and holes to generate light.

Figure 1 shows a plot of the energy band gap as a function of lattice constant for several III-V semiconductors. The lines that connect points on the graph show how the band gap and the lattice constant vary for mixtures of the binary compounds to which the points correspond. For example, the ternary compound $Ga_xAl_{1-x}As$, which is closely lattice-matched to GaAs, can be made to have a band gap between 1.4 and 2.2 eV by varying the ratio of gallium to aluminum. The difference in the band gap can be used to confine light and carriers in a $GaAs/Al_xGa_{1-x}As$ heterostructure. Quaternary compounds (Q), such as $In_xGa_{1-x}As_yP_{1-y}$, can be lattice matched to InP and have band gaps in the wavelength range of 1.3 to 1.6 μm, which is the range such that light loss from silica-glass fibers (used in fiber-optic communication) is low. Also shown in Fig. 1 are the lattice constants and band gaps of elemental silicon and germanium. Silicon has the smallest lattice constant of the semiconductors shown. Thin-film epitaxy on its surface is only possible through the generation of large compressive stresses that cause the alloy layer to deform and thus match the atomic spacing of the substrate.

Fabrication of Layered Heterostructures

Great advances in the fabrication of layered heterostructures have taken place in recent years. Among the techniques that have been used are liquid-phase epitaxy (LPE), chemical vapor deposition (CVD), and molecular-beam epitaxy (MBE). In LPE the epitaxial layer is grown by cooling a heated metallic solution that is saturated with the components needed to grow the layer and that is kept in contact with the substrate. In CVD the epitaxial layer is grown from a heated source of gaseous elements or compounds that react at the substrate surface. Considerable progress has been made in the growth of quantum well heterostructures with metal-organic chemical vapor deposition (MOCVD). Metal alkyls are used as the compound source. In MBE the deposition occurs under controlled

The author is director of the Solid State Electronics Research Laboratory at AT&T Bell Laboratories, Murray Hill, NJ 07974.

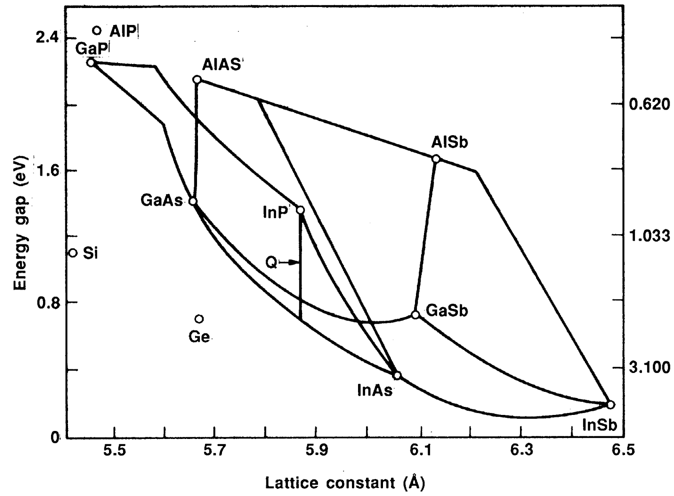

Fig. 1. A plot of the energy gap versus lattice constant for several III-V semiconductors. The lines that connect points on the graph show how the band gap and the lattice constant vary for mixtures of the binary compounds and for quaternary compounds (Q) to which the points correspond. Also shown are the band gap and lattice constant for the elemental semiconductors silicon and germanium.

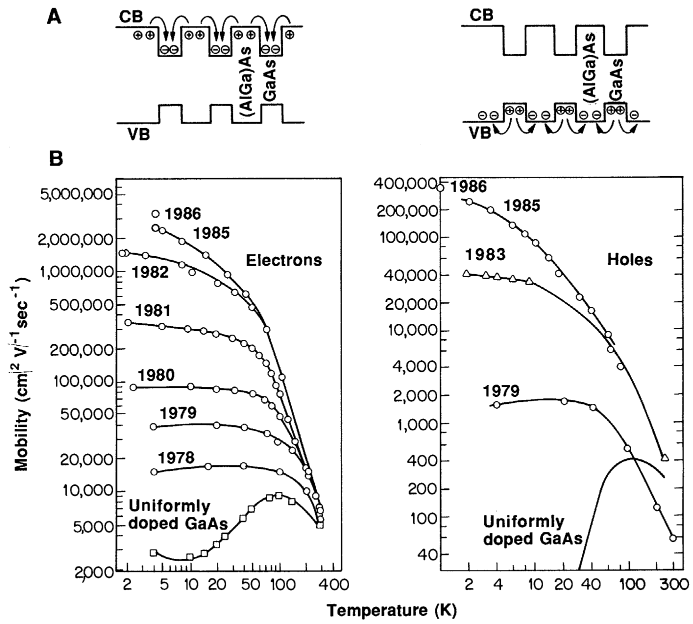

Fig. 2. (**A**) Schematic illustration of modulation doping for electrons and holes. (The conduction and valence bands are indicated as (CB and VB.) (**B**) Highest reported electron and hole mobilities as function of temperature during the period 1978 to 1986 (compiled by A. C. Gossard).

ultrahigh vacuum conditions. Crystal growth results through the reaction of one or more thermal beams of atoms and molecules of the constituent elements with a crystalline substrate held at a suitable temperature. The growth is monitored through in situ surface diagnostic tools, such as low-energy electron diffraction (LEED). The clean environment, the slow growth rate, and the independent control of the beam sources allow the precise fabrication of atomic scale semiconductor heterostructures.

The clear distinctions among the growth techniques have recently begun to fade, and new techniques have appeared. In the case of III-V compound semiconductors, the high vapor pressure of the group V sources, particularly phosphorus, has led to the development of gas-source MBE (GSMBE). In this hybrid technique (*4*), the gases AsH_3 and PH_3 are passed through a thermal, catalytic cracker oven and then introduced into the vacuum chamber through a controlled leak. In this way a stable beam intensity is obtained. For growth of InGaAsP, precise control of the mix of arsenic and phosphorus is possible. In a further variant (*5*) of GSMBE the group III elements are organometallic compounds as in MOCVD. Hybrid methods that use the advantages of an ultrahigh vacuum environment and of gaseous sources will likely become the techniques of choice.

Progress in these crystal growth techniques has allowed the construction of atomic scale structures that can have virtually arbitrary potentials for electrons and holes. These potentials include abrupt band discontinuities, which are used to confine carriers in a two-dimensional (2-D) state. Because of their applications to novel and potentially useful devices, the physics of thin-film semiconductor heterostructures has become a subject of intense study.

High Carrier Mobility Structures

The principal building block of silicon integrated circuits (ICs) is the metal-oxide field-effect transistor (MOSFET), which can be described simply as a layer of 2-D electrons (holes) confined to the interface between crystalline silicon and its native oxide (SiO_2). In the case of GaAs, the inversion layer can be formed at the interface of a GaAs/$Al_xGa_{1-x}As$ heterostructure. Until 1978, carrier mobilities in such structures were extremely low. At that time Stormer and his colleagues introduced modulation doping (*6*), in which the band-edge discontinuity in the heterostructure is used to separate the electrons (holes) from their parent donors (acceptors), as shown in Fig. 2A. This results in greatly enhanced mobilities (μ) when compared with uniformly doped materials. The greatest improvement in the mobility is found at low temperatures, where scattering from ionized impurities is the dominant mechanism for reducing mobility in uniformly doped materials. Even at room temperature, modulation-doped structures show an enhancement in mobilities over a uniformly doped material, in spite of the fact that at higher temperatures thermal phonon scattering becomes progressively more important.

Figure 2B shows a plot of the electron and hole mobility that could be achieved with modulation-doped structures during the period 1978 to 1986. The steady improvement in the mobility that could be achieved can be traced to (i) the introduction of an undoped spacer layer adjacent to the barrier layer that further separates the parent donors (acceptors) from the electrons (holes); (ii) the use of a modulation-doped single interface instead of a superlattice; and (iii) improvements in growth techniques, such as the introduction of a sample load lock to prevent contamination of the main growth chamber during introduction of the sample. The achievement of high carrier mobilities has led to the observation of novel quantization phenomena (the fractional quantum Hall effect) for 2-D electron and hole systems (*7*).

Modulation doping causes greatly enhanced conductivity in the plane of the layered structure as compared to that in the direction perpendicular to the layers. This effect is exploited in the modulation-doped field-effect transistor (MODFET). These devices are characterized by high switching speeds and low power consumption. At 77 K, where the modulation doping advantage is already significant, a switching time as short as 5.8 psec has been observed (*8*). Such transistors will probably form the basis of advanced GaAs digital circuits. A 4-kilobit static random access memory (RAM) and a high-speed multiplier have been fabricated. The recent demonstration of high-mobility holes has led to the fabrication of low power, complementary (*n*- and *p*-type) transistor circuits in the GaAs system.

Quantum States, Perpendicular Transport, and Tunneling

Quantum wells in GaAs with thicknesses of a few hundred angstroms can result in the quantum confinement of electrons. These quantum states were observed in 1974 at low temperatures in electron transport through resonant tunneling (*9*) and through optical absorption (*10*) at well-defined energies. The quantum confinement also causes modification of the electronic density of states and has led to the observation of several novel effects, such as room temperature exciton absorption and low-threshold semiconductor lasers.

An example of a structure which illustrates the effects of perpendicular resonant tunneling is shown in the upper part of Fig. 3, which is a schematic of the first room temperature (*11*) resonant tunneling bipolar transistor (RTBT). The wide band-gap $Al_x Ga_{1-x}As$ emitter is graded (*12*) by chopping the beam from the aluminum effusion cell over a distance of about 500 Å to a value of $x = 0.07$, so that the energy difference between the emitter electrons and the first quantum state in the base of the transistor is near the thermal energy of the electrons. The base itself consists of a 74-Å undoped GaAs well with 21.5-Å AlAs barriers. Electrons are thermally injected into and transported through the base. The collector current (I_c) (at a fixed collector-emitter voltage) increases with a gain of ~5 as a function of base current (I_b) for $I_b < 2.5$ mA, which is a normal characteristic of a bipolar transistor. At higher base currents the current gain is quenched approximately exponentially as a result of the suppression of resonant tunneling, because the conduction band edge of the $Al_{0.07}Ga_{0.93}As$ is above the first energy level of the quantum well. In the region of negative transconductance, the RTBT behaves as an oscillator. The number of possible (*13*) transistors with unique functions is large. Through careful design of structures with several resonant states in the base, it should be possible to fabricate bipolar transistors with multiple stable states.

Gas-Source MBE and Quantum Wells in InGaAsP

There has been significant progress in the growth of heterostructures and quantum wells on InP with the use of GSMBE and low-pressure MOCVD. The entire Q range of quaternary compositions (see Fig. 1) of $Ga_xIn_{1-x}As_yP_{1-y}$ on InP of interest for 1.3 to 1.6 μm fiber-optic transmission and heterostructure electronic devices, such as optical modulators and detectors, have been grown.

The degree of control (*14*) that has been achieved in crystal growth is revealed with the transmission electron microscope (TEM) image shown in Fig. 4. Micrographs of four $Ga_{0.47}In_{0.53}As$ quantum wells with thicknesses of 6, 9, 12, and 24 Å separated by InP barriers (which are ~150 Å thick) show that there are fluctuations of about one monolayer at the layer interfaces. Similar results were obtained with the quaternary quantum wells, although in that case the interfaces seem even more abrupt. Figure 4 shows measurements of low-temperature photoluminescence of these single quantum wells after illumination with light of higher energy than the band gap (632 nm, or 1.95 eV). The figure illustrates the enormous quantum size effect in the quantum well emission compared to that of bulk InGaAs (~1.6 μm) which for the thinnest wells (6 Å) corresponds to a shift in energy ΔE of 550 meV. For the 6-Å well the wavelength of emission is about 0.94 μm. Thus, by choosing wells of different thicknesses, one can make quantum well laser structures that span a wide wavelength range. The optical data also suggest a high degree of structural perfection (monolayer abruptness).

Lateral Quantum Confinement

MBE has been primarily used to provide quantum-confined structures in the direction of growth. Confinement in one and zero dimensions (quantum wires and quantum boxes) requires fabrication of laterally confined structures on a scale of about 100 Å. Such laterally confined structures can in principle be made by lithographically patterning the transverse dimensions of a quantum well structure grown by MBE. Such dimensions are at the present limits of electron-

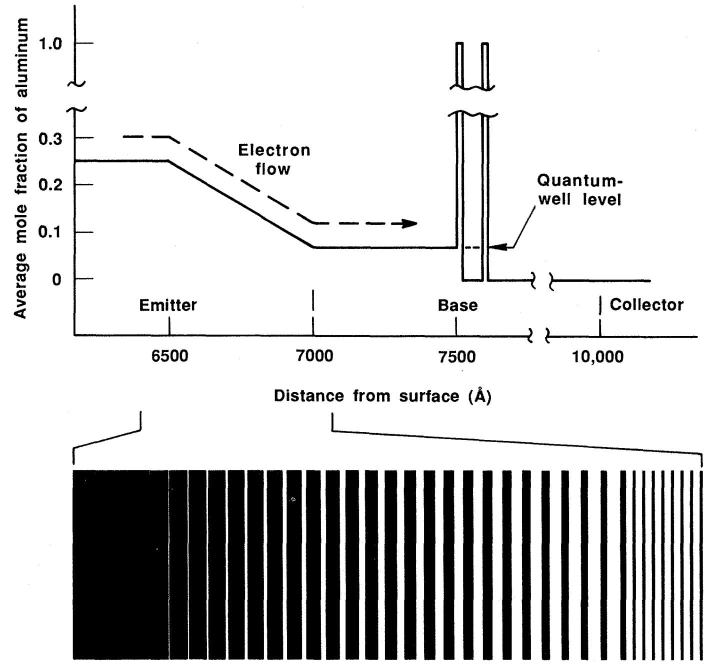

Fig. 3. Resonant tunneling bipolar transistor (RTBT) in the GaAlAs system grown by MBE. The aluminum composition of the emitter is graded by chopping of the effusion cell so that the average composition changes smoothly from a value of 0.25 to 0.07 and so that the emitter electrons are in resonance with the first quantum level in the base (*11*).

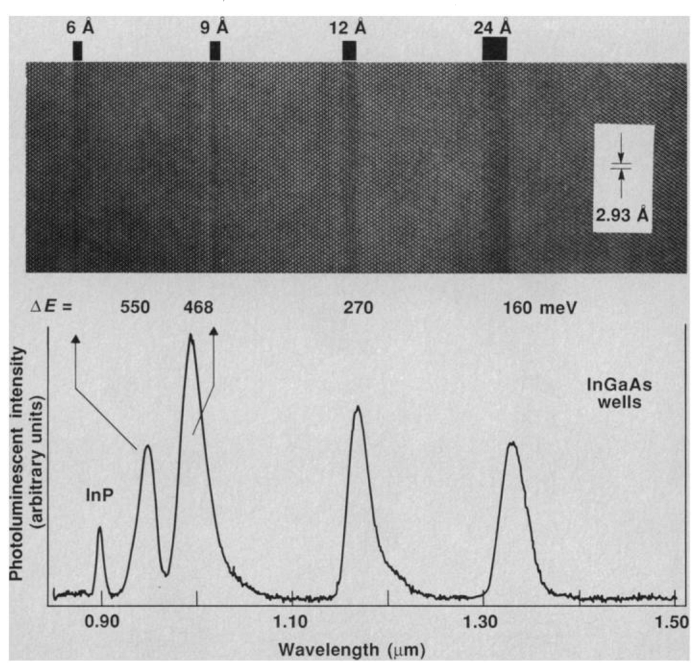

Fig. 4. Transmission electron microscope image of InGaAs quantum wells of thickness 6, 9, 12, and 24 Å separated by 150-Å InP barriers. The bottom shows photoluminescence spectra taken at 6 K of the quantum wells. The shift ΔE is measured from the known energy gap of bulk InGaAs (*14*).

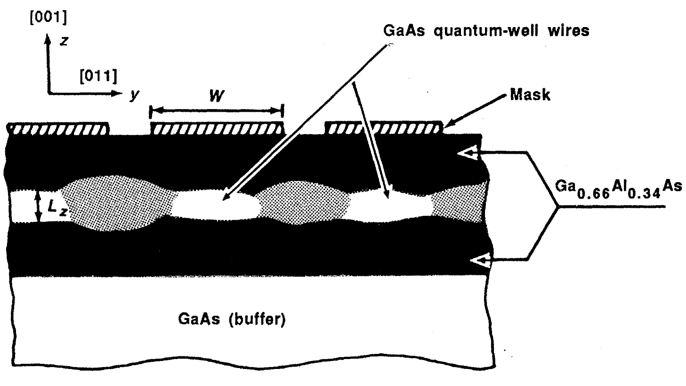

Fig. 5. Schematic (not to scale) of GaAs quantum well wire structure after implantation and annealing. The position of the mask (which has a width W) during implantation is indicated. The wires (which have a thickness L_z) are actually 1 μm apart (*15*).

beam lithography. In small structures the ratio of surface to volume is large and the patterning must be such that it does not degrade the sidewalls of the layers. Because of modification of the electronic density of states in these confined structures, several novel optical effects, such as an improvement in the performance of quantum wire semiconductor lasers, have been theoretically predicted.

Progress has been made in fabricating such structures in both the GaAs/AlGaAs and the InGaAs/InP systems. Cibert *et al.* (*15*) have fabricated quantum wires and boxes. They used gallium ions to disorder local areas of a GaAs/AlGaAs quantum well structure (see Fig. 5). The ion implantation occurred through open areas of an electron beam–defined tungsten mask. They discovered that the interdiffusion of aluminum in GaAs after a rapid thermal anneal is much larger in the disordered region than in the masked region. Thus they were able to produce high-quality laterally confined structures, in which new optical transitions that correspond to the theoretically predicted energy levels for quantum wires and boxes were observed.

An interesting case for the study of lateral confinement is the InGaAs/InP system. In this system the surface recombination velocity of electrons and holes is ~0.01 of that in the GaAs/AlGaAs system (*16*). Thus high luminescence efficiency may be expected. Temkin *et al.* (*17*) have fabricated quantum wires and boxes on the order of 300 Å in this system with electron-beam lithography. Figure 6A shows an electron micrograph of some typical quantum boxes with an average diameter of 300 (± 50) Å. Quantum wires with lateral dimensions ~300 Å have also been fabricated. Figure 6B shows typical photoluminescence spectra for these quantum structures. The luminescence shift of 8 to 14 meV is consistent with that expected for lateral dimensional confinement. The high photoluminescence efficiency is also consistent with the low surface recombination velocity that is characteristic of InP and its alloys.

Heteroepitaxy on Silicon

The use of silicon in semiconductor applications is ultimately limited by its incompatibility with other semiconductor materials. Silicon as a substrate material alone has attractive properties such as high mechanical strength, high degree of crystalline perfection, large diameters (~20 cm) to which it can be grown, natural abundance, and low cost. It is clear from Fig. 1 that if the electronic and optical properties of the silicon surface are to be altered through lattice-matched heterostructures, the number of possibilities are few. Both GaP and AlP, which are lattice-matched to silicon, are composed of elements that are commonly used as dopants in silicon. Thus, when crystal growth of thin films has been attempted, uncontrolled cross-doping effects (for example, interdiffusion of gallium or aluminum into the silicon) have resulted. Two major approaches have been used in heterostructure band-gap engineering on silicon. In the first, the elemental semiconductor germanium and its alloys Ge_xSi_{1-x} are grown. The idea is to use Si/Ge_xSi_{1-x} heterostructure single interfaces and superlattices for altering the band gap and hence the electronic and optical properties on the surface of silicon. In the second, silicon is used as a substrate material for growth of $GaAs/Al_xGa_{1-x}As$ heterostructure devices. This approach combines

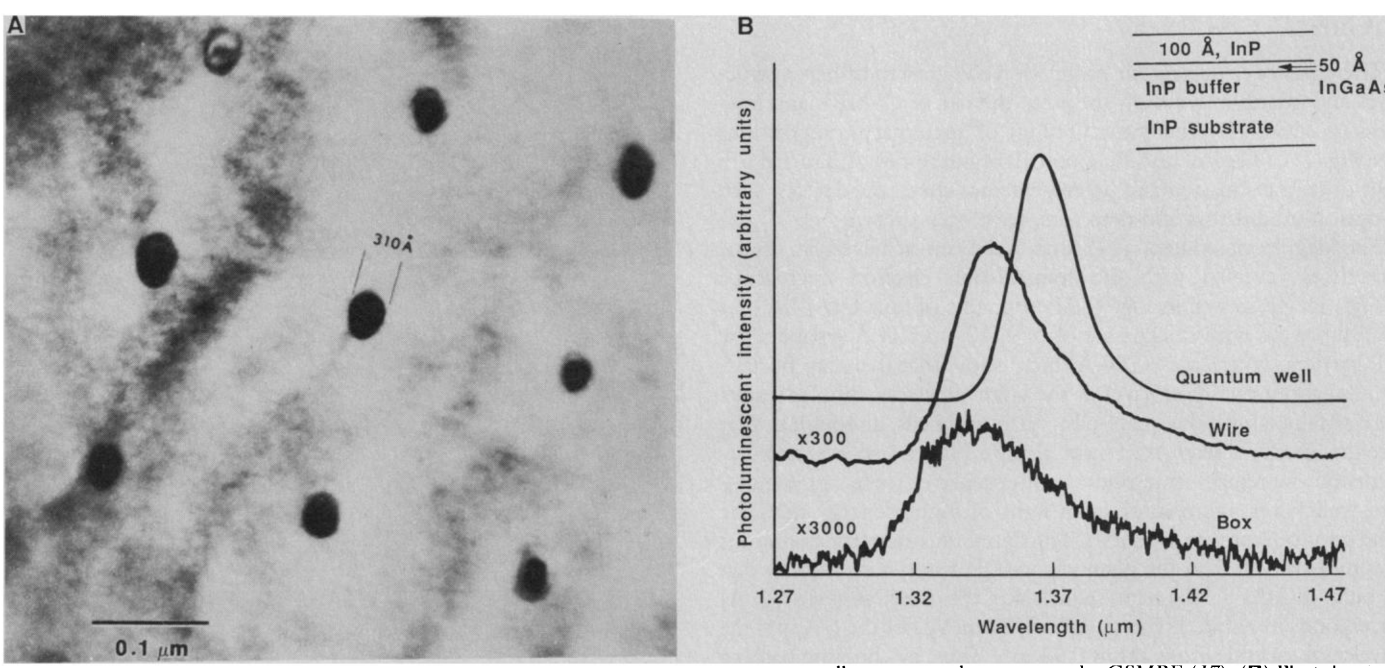

Fig. 6. (**A**) The transmission electron micrograph shows InGaAs/InP quantum boxes that were fabricated by direct electron-beam writing and ion-beam milling. The average box diameter is 300 Å. The initial 50-Å InGaAs quantum well, upper panel, was grown by GSMBE (*17*). (**B**) Photoluminescence of control quantum well sample, and for lithographically patterned 300-Å quantum well, wires, and boxes. The wires and boxes have thicknesses of ~300 Å.

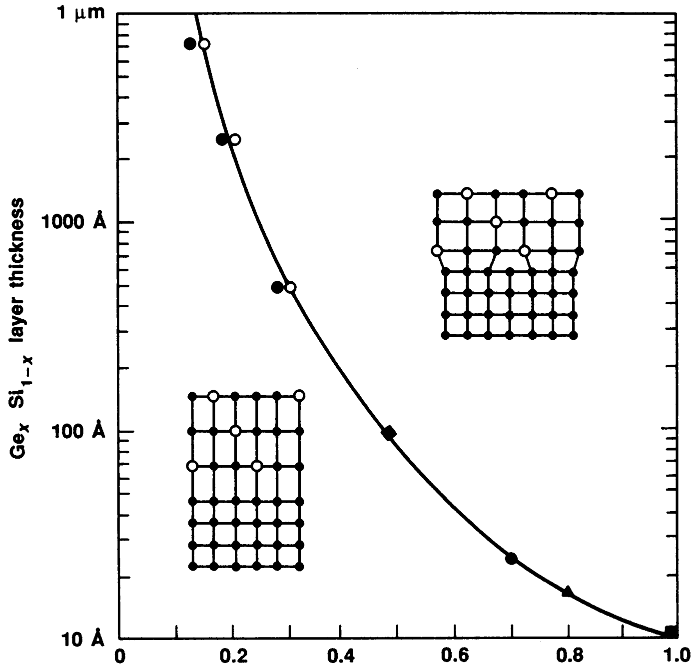

Fig. 7. Plot of critical film thickness for commensurate epitaxy as a function of x for Ge_xSi_{1-x} alloys grown on silicon substrates. The insets show the atomic arrangements for the strained but defect-free material found in sufficiently thin layers and for the bulk material in which misfit dislocations accommodate the lattice mismatch. [Adapted from (*18*)]

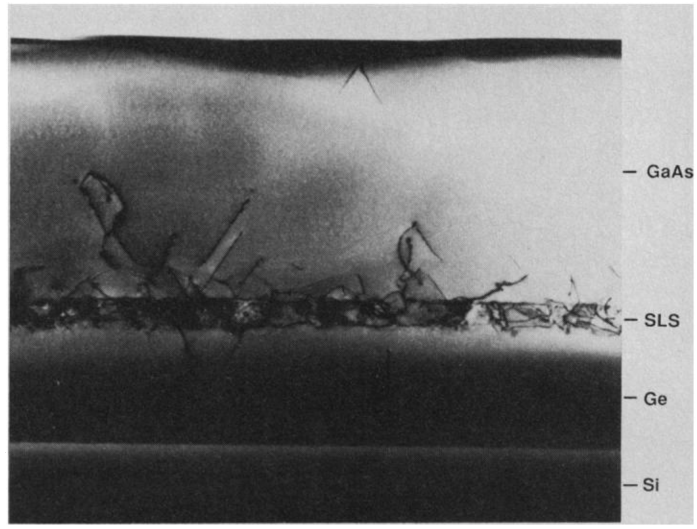

Fig. 8. Transmission electron micrograph of a GaAs/GaAs-GaAsP SLS structure grown on Ge/Si composite substrate. The GaAs layer is 2 μm thick. The germanium film on silicon was grown by MBE, the GaAs and GaAsP were grown by MOCVD. [Adapted from (*20*)]

the excellent properties of silicon as a substrate material with the unique electronic and optical properties of GaAs/AlGaAs heterostructures.

Although germanium has the same crystal structure as silicon, its lattice constant is approximately 4% larger. The epitaxial growth can occur either as incommensurate or as commensurate epitaxy. In the former (upper inset of Fig. 7), both crystals retain their individual structure; at the interface of germanium and silicon, every 25th row of atoms will have only three bonding neighbors. Rows of these improperly bonded atoms form "misfit dislocations" that can seriously degrade the electronic properties of the interface. In commensurate epitaxy (bottom inset, Fig. 7), the fourfold bonding at the interface is preserved by compression of the larger germanium lattice along the interface and by elongation perpendicular to the interface. Such strained-layer epitaxy is possible if the stored strain energy in the film is lower than the reduction in the dangling bond energy.

Heterostructures of Si/SiGe have been grown by MBE by Bean (*18*). Figure 7 shows a plot of the thickness of Ge_xSi_{1-x} alloys on silicon for commensurate epitaxy. The observed thicknesses for commensurate epitaxy are about ten times as large as those predicted by equilibrium theories of dislocation formation. The band gap of the strained GeSi films is considerably smaller than that of corresponding bulk alloys. The growth of GeSi heterostructures on silicon thus allows one to exploit "band-gap engineering" techniques for the production of novel, long wavelength photodetectors and MODFETs with silicon-based technologies.

The other approach is heteroepitaxial semiconductor (GaAs) growth on silicon (*19*). Like germanium, GaAs also has a lattice constant some 4% larger than that of silicon. GaAs is a polar semiconductor with a zinc blende structure. Thus, in addition to misfit dislocations, one must contend with control of additional structural defects such as antiphase domains. An antiphase domain is a region of the crystal where the nearest-neighbor bond is not between a gallium atom and an arsenic atom but is between two gallium atoms. The formation of such antiphase domains can be minimized by using misoriented silicon substrates. A silicon surface that is cut a few degrees off the ⟨100⟩ direction has a predominant number of double atomic steps (steps whose height is twice that of a single atomic step). Growth on such surfaces leads to a material that is free of antiphase domains.

In order to grow thick layers of GaAs on silicon with a low dislocation density, researchers have tried several other approaches besides misoriented substrates. In one approach (*20*) a germanium film (which has approximately the same lattice constant as GaAs, see Fig. 1) is grown by MBE. A GaAs/GaAsP strained-layer superlattice (SLS) is then grown by MOCVD, over which a thick GaAs film is grown (see Fig. 8). It is clear from the transmission electron microscope (TEM) image in Fig. 8 that the SLS appears to have trapped dislocations that may have moved from the germanium layer during the growth of the GaAs layer. The apparent dislocation density of these films at the surface is low ($\sim 10^4$ to $\sim 10^5$ cm^{-2}). Such structures have been used to grow GaAs/AlGaAs double heterostructure lasers that have low current thresholds. These lasers are not yet as good as those grown directly on GaAs substrates, but the progress in the growth of such structures, which are extremely sensitive to dislocation, has been remarkable.

MBE also allows the growth of compatible metals, such as silicides and insulators, on silicon. A buried heterostructure (*21*) of $Si/CoSi_2Si$ has been grown that demonstrates transistor action with the metal laser as a base. Epitaxial fluorides (*22*) on silicon have been used both for dielectric isolation and for the fabrication of field-effect transistors (FET). Most recently, ordered monolayer structures (*23*) of germanium on silicon have been grown, which represent another class of new materials on silicon.

The possibilities opened by heteroepitaxy with MBE are many and have only just begun to be explored. The low growth temperature and control permitted by MBE are unparalleled and will permit much further development in the area of heteroepitaxy.

Characterization of Interfaces and Thin Films

The surface and interface characterization of MBE-grown films has been of major importance in understanding the early stages of crystal growth and lattice formation. The earliest advances were

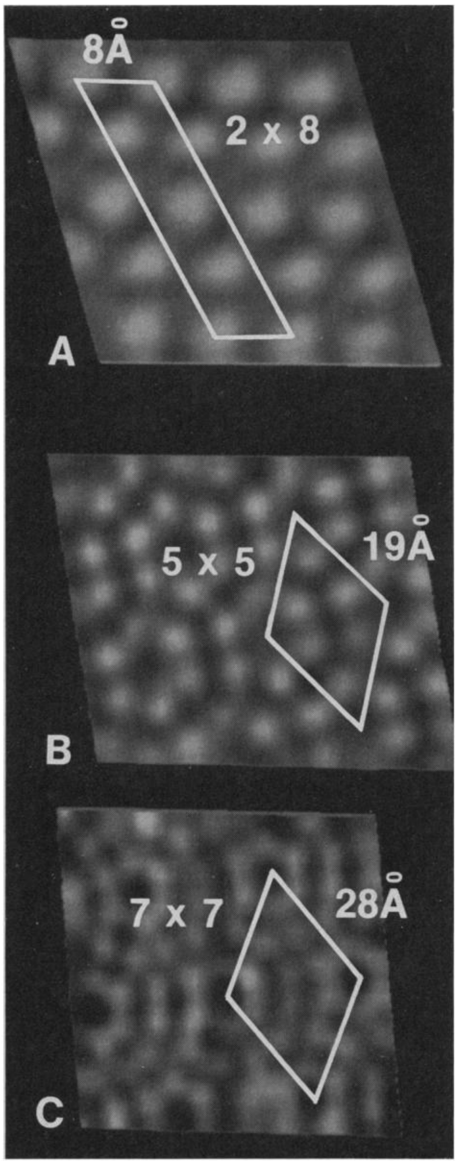

Fig. 9. Scanning tunneling microscopy images of germanium and GeSi on silicon grown by MBE and with different heat treatments. (**A**) The c(2 × 8) reconstruction for germanium on silicon, which is the normal reconstruction for clean germanium. (**B**) The newly observed (5 × 5) reconstruction for a 50:50 alloy of GeSi. This image also shows indications of ordering. (**C**) The (7 × 7) reconstruction, which is typical of clean silicon. [Adapted from (*27*)]

made with in situ LEED. More recently, powerful analytical techniques such as high-resolution TEM (HRTEM), x-ray scattering, and Rutherford backscattering have been used to characterize the degree of perfection of thin-film heterostructures. Often the results of a variety of techniques must be combined to obtain a complete picture. I have highlighted electron microscopy, which gives excellent visual images of the degree of perfection of thin-film interfaces and their structure.

Another microscopic technique that gives detailed and direct information of interface structure is the recently developed scanning tunneling microscope (STM) of Binnig *et al.* (*24*). The STM measures the very small current that flows when a potential is applied between the surface and a probe tip that is scanned across the interface at a distance of only a few angstroms. The quantum mechanical tunneling current is extremely sensitive to the distance between atoms on the surface and the tip, and serves as a direct method of observing individual atoms at interfaces. The STM has recently been used by Golovchenko and co-workers (*25*) to obtain the first images of atomic steps and their structure on silicon surfaces. They have also imaged the strain-stabilized crystal structure of germanium and GeSi grown by MBE on silicon surfaces.

LEED studies (*26*) showed that germanium epitaxially grown on silicon has a wide variety of reconstructions that depend on heat treatment. The STM images (*27*) shown in Fig. 9 provide the first detailed atomic scale images of the Ge c(2 × 8), GeSi (5 × 5), and Ge (7 × 7) reconstructions in silicon. (These are lattice symmetry designations.) These results show the remarkable detail of the surface structure and have helped to resolve many outstanding questions on the relation between clean germanium and silicon surface reconstructions. Of particular interest is the observation of the GeSi (5 × 5) reconstruction that has a rhombohedral unit cell with a lattice constant of 19.2 Å. The asymmetry between the two halves of the unit cell is clearly visible and suggests that an ordered alloy with alternate positions around the deep depressions exists on the surface.

These studies, like many of the other cited in this article, are still in their infancy. It is probable that future MBE machines will have capability for in situ studies of crystal growth by the most powerful characterization techniques, such as STM and HRTEM. If recent history is any guide, it is likely that such studies will lead to entirely new classes of materials as a fuller understanding is developed of the first stages of crystal growth.

REFERENCES AND NOTES

1. A. Y. Cho, *Thin Solid Films* **100**, 291 (1983); R. D. Dupuis, *Science* **226**, 623 (1984).
2. For a recent review, see V. Narayanamurti, *Phys. Today.* **37** (no. 10), 24 (1984).
3. C. M. Falco, in *Festkorperprobleme, Advances in Solid State Physics* **25**, 531 (1985).
4. M. B. Panish, *J. Electrochem. Soc.* **127**, 2729 (1980); for a review, see M. B. Panish, in *Proceedings of 1986 York Molecular Beam Epitaxy Conference*, to be published in *J. Cryst. Growth* (in press).
5. W. T. Tsang, *Appl. Phys. Lett.* **45**, 1234 (1984).
6. For a review, see H. L. Stormer, *Surf. Sci.* **132**, 519 (1983).
7. ——— and D. C. Tsui, *Science* **220**, 1241 (1983).
8. N. J. Shah, S. S. Pei, C. W. Tu, R. C. Tiberio, *IEEE Trans. Electron Devices* **ED-33**, 543 (1986).
9. L. L. Chang and L. Esaki, in *Molecular Beam Epitaxy*, B. R. Pamplin, Ed. (Pergamon, Oxford, 1980), p. 15.
10. R. Dingle, in vol. 15 of *Festkorperprobleme*, H. J. Queisser, Ed. (Pergamon, Oxford, 1975), p. 21.
11. F. Capasso, S. Sen, A. C. Gossard, A. L. Hutchinson, J. H. English, *IEEE Electron Device Lett.* **EDL-7**, 573 (1986).
12. A. C. Gossard, *IEEE J. Quantum Electron.* **22**, 1649 (1986).
13. F. Capasso, *Science* **235**, 172 (1987).
14. M. B. Panish, H. Temkin, R. A. Hamm, S. N. G. Chu, *Appl. Phys. Lett.* **49**, 164 (1986).
15. J. Cibert *et al.*, *ibid.*, p. 1275.
16. H. C. Casey and E. Buehler, *ibid.* **30**, 247 (1977).
17. H. Temkin, G. J. Dolan, M. B. Panish, S. N. G. Chu, *ibid.*, in press.
18. J. C. Bean, *Science* **230**, 127 (1985).
19. S. L. Wright, H. Kroemer, M. Inada, *J. Appl. Phys.* **55**, 2916 (1984); T. H. Windhorn and G. M. Metze, *Appl. Phys. Lett.* **47**, 1031 (1985); R. Fischer, W. Kopp, H. Morkoc, *ibid.* **48**, 1360 (1986).
20. R. D. Dupuis *et al.*, *J. Electron. Mater.*, in press.
21. J. C. Hensel, A. F. J. Levi, R. T. Tung, J. M. Gibson, *Appl. Phys. Lett.* **47**, 151 (1985).
22. T. P. Smith III, J. M. Phillips, W. M. Augustyniak, P. J. Stiles, *ibid.* **45**, 907 (1984).
23. J. Bevk, J. P. Mannaerts, L. C. Feldman, B. A. Davidson, A. Ourmazd, *ibid.* **49**, 286 (1986).
24. G. Binnig, H. Rohrer, C. Gerber, E. Weibel, *Phys. Rev. Lett.* **50**, 120 (1983).
25. For a review, see J. A. Golovchenko, *Science* **232**, 48 (1986).
26. H. J. Gossman, J. C. Bean, L. C. Feldman, E. G. McRae, I. K. Robinson, *J. Vac. Sci. Technol.* **A3**, 1633 (1985).
27. R. S. Becker, J. A. Golovchenko, B. S. Swartzentruber, *Phys. Rev. Lett.* **54**, 2678 (1985); *Phys. Rev.* **B32**, 8455 (1985).
28. I thank the following colleagues for help with the preparation of this article: J. C. Bean, R. S. Becker, F. Capasso, A. Y. Cho, R. D. Dupuis, A. C. Gossard, M. B. Panish, P. M. Petroff, H. L. Stormer, and H. Temkin.